

# Scanning Parameter Selection for Inkjet Print Analysis

*Jennifer C. Stanek and Peter D. Burns  
Eastman Kodak Company  
Rochester, New York*

## Abstract

Noise in inkjet prints can be influenced by many factors, such as halftone pattern, dot size, dot color and ink coalescence. The measurement of various image noise characteristics, such as random graininess and banding, is often needed as part of system design and optimization.

We consider the imaging requirements for a scanner used for inkjet printer evaluation. Methods to assess the influence of print sampling, scanner MTF, and noise characteristics are addressed, and applied to an application of print granularity assessment.

## Introduction

While microdensitometers have historically been used to measure image microstructure, it is now common for desktop scanners to acquire image data for this purpose.<sup>1-3</sup> This can place demands on the scanner performance, position accuracy, noise, etc., which are beyond its capability. While this may not be a serious problem if a practical relative measurement is needed, comparing results between systems and laboratories is difficult. Our primary objective was a visually weighted graininess measure. The approach taken, however, is intended to be general and applicable to systems for measurement of printer MTF, line quality, low-frequency mottle, etc.

A method to assess the influence of scanner sampling, MTF and noise characteristics will be addressed. This leads to both selection of a desktop scanner, and its operating conditions such as sampling, signal processing and encoding. Figure 1 shows the elements of a scanner that can influence the imaging characteristics, and therefore are important to the measurement of image microstructure.

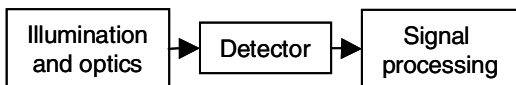


Figure 1. Elements of scanner

The illumination, optics and image detector would appear, at first, to determine the imaging performance of a digital scanner. The selection by the user of software driver settings, however, determines several signal processing

steps that influence performance. A simple selection of image sampling of, for example, 400 or 600 pixels per inch (ppi) implies a spatial processing from the native detector data to the delivered image, which may be neither of these settings. Setting of contrast or "gamma" setting in a software driver invokes a look-up table that influences both signal quantization and detector noise propagation.

Our approach to understanding imaging requirements for inkjet print evaluation, and selection of operating parameters, is to evaluate the effective scanner MTF, noise sources, and signal quantization. This needs to be done in the context of the color signal processing path.

## Scanner Measurements

### MTF

The level of detail needed for the measurement sets the measurement system MTF and sampling requirements. We used a well-established slanted-edge method,<sup>4</sup> and corrected for the spatial frequency response of the photographic target edge. Results for our Umax scanner is shown in Fig. 2 for 800 ppi (or dpi) sampling.

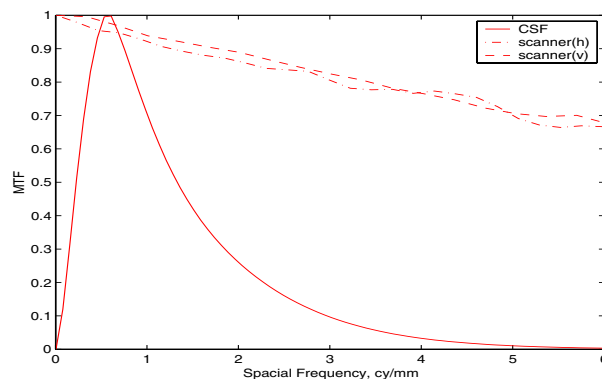


Figure 2. Comparison of scanner MTF and CSF

Because we are dealing with samples for direct viewing, the range of spatial frequencies of visual importance for continuous-tone image information is usually taken as dictated by an appropriate visual contrast sensitivity function. This range, approximately 0-5 cy/mm for most tasks, can be compared with the measured system

MTF performance. An example achromatic visual weighting<sup>3</sup> for 30 cm viewing distance is also shown in Fig. 2. These results indicate the small correction that would result from compensation for the scanner MTF, prior to application of the frequency weighting of a contrast sensitivity function (CSF).

### Scanner Noise

Because digital scanners and printers are subject to both random and non-random noise sources,<sup>6,7</sup> identification of both the rms noise level and its frequency components is advisable. The results of a noise-power spectrum analysis, following a separation of fixed-pattern noise<sup>7</sup> is shown in Fig. 3. A detailed description of methods for reliable NPS measurement<sup>8,9</sup> will not be presented here. An important step to include, however, is the removal of trends in the data, whose presence inflates important low-frequency estimates. We have found that estimation of both the two-dimensional NPS and its (inverse) Fourier-transform, the autocovariance function, is useful in the examination of noise sources in printed images.

Figure 3 shows the results for a uniform, low-noise gray photographic sample. For this application, scanner noise was not a serious problem. Note, however, that the image noise contribution of the scanner should be evaluated using the same signal path as the scanned print data. In this case, the units are variance per spatial frequency squared. Because this analysis was done for the CIELAB lightness signal, we can write this as  $L^* mm^2$ .

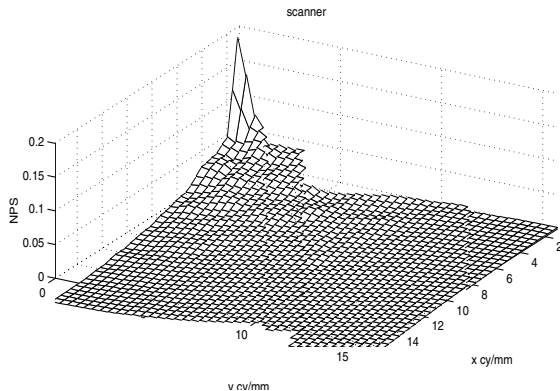


Figure 3. Example low-noise target and scanner noise-power spectrum

### Print Measurement Procedure

Optical density fluctuations of a material are often described by an rms granularity measure. An observer's perception of granularity is referred to as graininess. Our objective was to develop a method for reliable visually weighted noise (graininess) measurement based on a CIELAB lightness signal.

Although image noise of inkjet prints is mainly a function of the halftone pattern, it is also dependent on the composite color inks. Many different combinations of

cyan, magenta, yellow and black ink can be used to produce the same composite (mean) color. Often some combinations of the four inks are significantly noisier than other combinations even though the composite color is the same.

As a result of the metameric nature of inkjet systems, it is not wise to assume a single transformation from scanner code values to the CIELAB color space. Scanner characterizations should be made for each type of printing system. A general overview of the measurement and analysis chain is shown in Fig. 4.

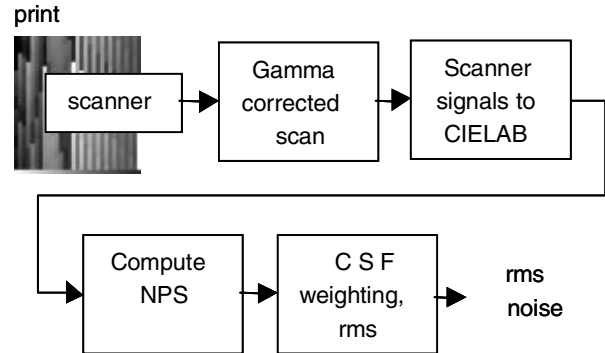


Figure 4. Outline of measurement and analysis

The first three steps of Fig. 4 comprise the scanner color characterization. A color-profile building target with 424 different colors was printed on a Kodak Professional large format 3062 inkjet printer. The CIELAB coordinates of each color were measured with a Gretag Spectrolino spectrophotometer, and the target was scanned on the flatbed scanner. The following scanner control parameters were set in the driver software,

<b>Scan Source:</b>	Flatbed (Reflective)
<b>Scan Mode:</b>	RGB
<b>Highlight:</b>	255
<b>Shadow:</b>	0
<b>Descreen:</b>	No descreen
<b>Gamma:</b>	2.4

It is important to note that the manual scanning mode should be used when making this type of measurement, to avoid any unwanted auto-scaling of the signal encoding.

The *gamma* setting is also called a *gamma correction* for a CRT display. The value of 2.4 was used; this resulted in a low-contrast, light image when displayed on the computer monitor, but minimizes the subsequent quantization introduced in the transformation from scanner signals to CIELAB. This is because our scanner implements the *gamma* transformation as a 14-bit to 8-bit look-up table (LUT). The  $L^*$  values were based on modified  $r, g, b$  signals, as shown in Fig. 5.

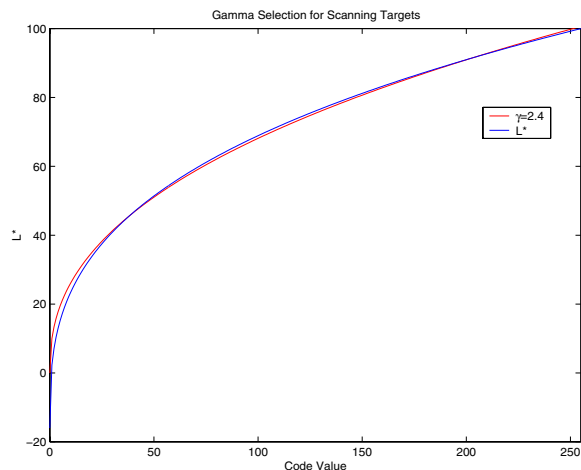


Figure 5. Comparison of scanner "gamma" response and  $L^*$  calculation from  $Y$ , where code value is taken as  $255 \cdot Y$ .

### Scanning Resolution and Sample Size Selection

The fourth step in the processing chain shown in Fig. 4 is the computation of the noise-power spectrum (NPS). This was done for each color patch on a color test target. The two dimensional noise-power spectrum was used to describe the image noise statistics of each sample. The NPS can be thought of as a spatial-frequency decomposition of the noise variance. The rms noise, granularity, is defined as the square root of the area under the noise-power spectrum curve.<sup>8</sup>

In order to compute the NPS, the sample patch size and scanning resolution were examined. Careful consideration was given to these two parameters to ensure that the image structure of each patch would be accurately represented in the frequency domain. If the scanning resolution is too low, the signal may be aliased. This is particularly true for printing with digital halftone patterns that introduce repetitive patterns.

The patch size must be large enough to provide an adequate number of samples ( $N$ ) for computing the noise-power spectrum. For a given sampling scheme, increasing the sample size, increases the frequency sampling of the resulting NPS estimate. A large patch size and high scanning resolution, however, will result in undesirably large file sizes and a coarse sampling of the printer color gamut since fewer larger patches fit on a printed target. We wanted to accomplish our characterization with one printed sheet.

To determine the optimal scanning resolution and target size, the noise-power spectra and rms granularity were evaluated for patch targets with varying number of samples ( $N$ ) scanned at several resolutions. Patch targets (5 cm square) were printed on the Kodak Professional large format 3062 inkjet printer at 720 dpi using the printer tone scale look up table without the ICC printer profile. Five CMYK composite halftoned colors were visually selected from a printed target. These five colors spanned the range

of perceived noise from very low to very high. The patches were scanned at 720, 800, 900, 1000, 1200 and 1440 dpi. For the noise-power spectrum calculations, the patches were digitally cropped into 5 sizes ranging from 1.0 to 2.5cm square. The color patches were scanned on the scanner using the same parameters previously listed for the color profile target. The scanner RGB code value to CIE  $L^*a^*b^*$  profile was applied and the noise-power spectrum and rms granularity of the  $L^*$  data were computed. Table 1 shows the rms granularity computed for all combinations of patch size and scanning resolution. At this point, there is no human visual system weighting factor.

Table 1. RMS Granularity of Patch Targets Scanned at various image sampling, and sample sizes. Units are rms  $L^*$ .

dpi	Sample size, cm (side)					
	1.02	1.27	1.52	1.78	2.03	2.54
720	5.08	5.04	5.03	5.02	5.00	5.01
800	5.52	5.48	5.45	5.44	5.43	5.46
900	5.69	5.63	5.61	5.60	5.58	5.58
1000	5.75	5.69	5.67	5.66	5.63	5.64
1200	5.80	5.74	5.72	5.70	5.68	5.68
1440	7.04	6.99	6.98	6.97	6.94	6.92

Looking across the columns in Table 1, it can be seen that the rms granularity is invariant for the range of sample patches sizes listed. To verify that a patch size of 2.5 cm square was sufficient, the rms granularity was computed for the entire 5 mm target. The granularity of the full patch was consistent with those from the other cropped sizes. Looking down the rows of Table 1, it can be seen that rms increases when the scanning resolution is increased from 720 to 1440 dpi. The rms is relatively consistent for the 800 to 1200 dpi scans.

In order to better understand the root of these differences, the noise-power-spectra were plotted. Figure 6 shows one quadrant of a one-dimensional slice through the two-dimensional noise-power spectrum of one patch color for six different scanning resolutions.

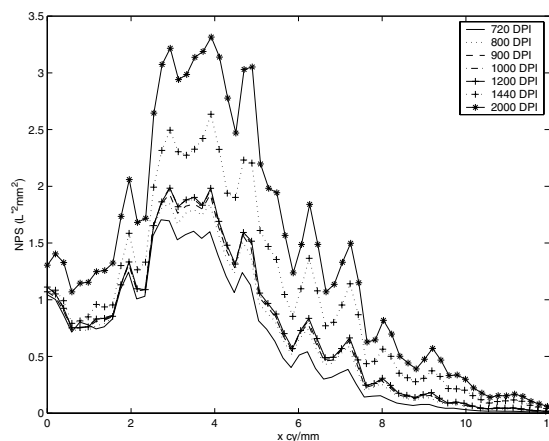


Figure 6. NPS estimate cross-section for various scanner sampling

In Fig. 6, all patches were 2 cm square (meaning that the 720 dpi patch was 576 pixels square, the 800 dpi patch was 640 pixels square, etc). It can be seen that the shape of the spectra remains consistent when the scanning resolution is reduced from 2000 to 720 dpi. The 2000 dpi scan had the highest power, the 720 dpi scan had the lowest, and the 800, 900 and 1200 dpi scans had virtually coincident power spectra. The spectra had negligible power at frequencies greater than 12 cycles/mm. Comparing the two-dimensional power spectra in Figures 7 and 8, it can be seen that the general shape of the spectrum sampled at 2000 dpi is maintained when the sampling resolution is reduced to 800 dpi. No significant aliasing components are seen.

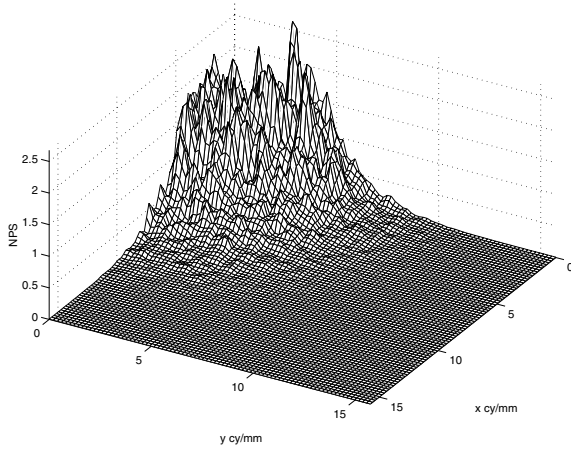


Figure 7. Example NPS for 800 dpi scanned data

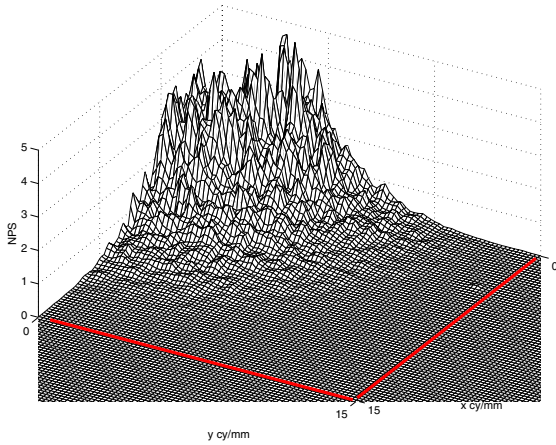


Figure 8. NPS for sample of Fig. 7 scanned at 2000 dpi.

From these plots, we conclude that sampling at a resolution higher than 800 dpi is not necessary. The difference in signal level seen between the higher and lower resolution scans may not be important for our application because we are concerned with the relative noise differences. While there are slight differences in the scanner MTFs for the differing sampling rates, these differences are not large enough to account for the observed NPS differences. A more likely explanation is the presence of non-random, or pseudo-periodic, fluctuations in the printed images. These noise components are a natural consequence of digital halftoning and printing, even when 'stochastic' methods, such as error diffusion,<sup>10</sup> are used. When periodic fluctuations are present, they introduce a bias into the NPS measurement, which is tailored to the measurement of random processes.<sup>6,11</sup>

### Computation of the CSF-Weighted Granularity

After weighting the noise-power spectrum of each patch with the human visual system contrast sensitivity function, the graininess measure is computed. For continuous rms granularity measurement, the measure is taken as the square root of the area under (two-dimensional integral of) the HVS-weighted noise-power spectrum. For discrete estimates based on sampled data, the integral is replaced by summation terms. Consider the NPS estimate in the form of an array,

$$n_{i,j}, i = 1, N, j = 1, M \quad (1)$$

and a corresponding CSF,

$$c_{i,j}, i = 1, N, j = 1, M, \quad (2)$$

where the indices correspond to spatial frequencies zero to the half-sampling frequency. The spatial frequency sampling of the estimate is determined by the original data sampling,  $\Delta x$ ,  $\Delta y$ , and the size of the NPS estimate array,

$$\Delta f_x = \frac{1}{2\Delta x(N-1)} \quad (3)$$

$$\Delta f_y = \frac{1}{2\Delta y(M-1)}$$

The CSF-weighted granularity is given by,

$$g = \left[ \Delta f_x \Delta f_y \left\{ n_{1,1} c_{1,1}^2 + n_{n,n} c_{m,m}^2 + 2 \sum_{i=2}^{N-1} n_{i,1} c_{i,1}^2 + 4 \sum_{i=2}^{N-1} \sum_{j=2}^{M-1} n_{i,j} c_{i,j}^2 \right\} \right]^{0.5} \quad (4)$$

When compared visually, the CSF-weighted granularity predictions calculated for sample prints corresponded reasonably well to the perceived noise. For example, if presented with the following three samples it is clear that sample *a*, having granularity, or rms, equal to 0.27 is much less noisy than sample *c* with rms equal to 6.67.

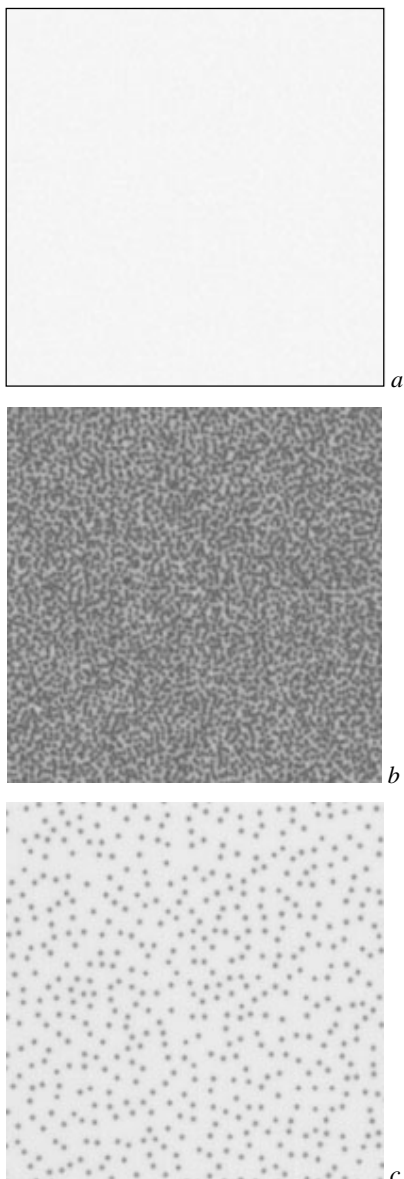


Figure 9. Scanned samples (see text for details)

## Conclusion

The imaging requirements for print evaluation can be addressed in a similar way to those for traditional microdensitometry. The level of spatial detail can be expressed in terms of MTF and sampling requirements. System noise characteristics, when analyzed through a path consistent with color signal processing can be expressed in terms of noise-power spectra, for comparison with anticipated sample noise levels.

Another important consideration is the sensitivity of results to scanning and signal processing parameters selections. Since the selection of scanning resolution usually implies spatial processing of the detected image data, analysis of an effective measurement MTF for

various settings is advisable. The presence of aliasing in a given measurement application, can be detected by comparing results for the same samples taken under varying measurement conditions.

## Acknowledgements

Many thanks to Doug Couwenhoven, Kevin Spaulding and Gus Braun for contributions to this work.

## References

1. W. Lim and S. Mani, Application of Digital Imaging to Measure Print Quality, *Proc. NIP 14 Conf.*, IS&T, pg. 611 (1998).
2. D. R. Rasmussen, B. Mishra and M. Mongeon, Using Drum and Flatbed Scanners for Color Image Quality Measurements, *Proc. PICS Conf.*, IS&T, pg. 108 (2000).
3. M. C. Mongeon, E. Dalal and R. Rasmussen, Utilizing Flatbed Scanners to Measure Printer Motion Quality Error, *Proc. PICS Conf. IS&T*, pg. 104 (2002).
4. P. D. Burns, Slanted-Edge MTF for Digital Camera and Scanner Analysis, *Proc. PICS Conf.*, IS&T, pg. 135 (2000).
5. S. Daly, in *Digital Images and Human Vision*, A.B. Watson, ed. pg.179, MIT Press, Cambridge, Mass., 1993.
6. P. J. Kane, T. F. Bouk, P. D. Burns, and A. D. Thompson, Quantification of Banding, Streaking and Grain in Flat Field Images, *Proc. PICS Conf.*, IS&T, pg. 79 (2000).
7. P. D. Burns and D. Williams, Distilling Noise Sources for Digital Capture Devices, *Proc. PICS Conf.*, IS&T, pg. 132 (2001).
8. J. C. Dainty and R. Shaw, *Image Science*. Academic Press, (1974).
9. J. Vranckx, P. Breesch and M. DeBelder, *Photogr. Sci. Eng.*, **28**, 134 (1985).
10. R. Ulichney, *Digital Halftoning*, The MIT Press, Cambridge, Mass., ch. 8, 1987.
11. P. D. Burns, Measurement of Random and Periodic Image Noise in Raster-Written Images, *Proc. Advances in Non-Impact Printing Tech.*, pg. 139 (1984).

## Biographies

**Jennifer Cerniglia Stanek** received a BS and MS in Imaging Science from Rochester Institute of Technology. She joined Eastman Kodak Company in 1996 as a Research Scientist, and is currently working in the Digital Input/Output Processing and Modeling Group. Her current research focuses on inkjet simulations and developing noise models.

**Peter Burns** studied Electrical and Computer Engineering at Clarkson University, receiving his BS and MS degrees. In 1997, he completed his Ph.D. in Imaging Science at Rochester Institute of Technology. After working for Xerox, he joined Eastman Kodak Company, where he works in Electronic Imaging Products R&D.